Climatic Change (2020) 162:603–619
https://doi.org/10.1007/s10584-020-02725-2

Greater probability of extreme precipitation under 1.5 °C and 2 °C warming limits over East-Central Asia

Meng Zhang[1,2] · Haipeng Yu[1,3] · Andrew D. King[4] · Yun Wei[2] · Jianping Huang[5] · Yu Ren[2]

Received: 7 June 2019 / Accepted: 27 April 2020 / Published online: 27 May 2020
© Springer Nature B.V. 2020, corrected publication 2020

Abstract

East-Central Asia is one of the most vulnerable and sensitive regions to climate change, and the variability of extreme precipitation attracts great attention due to the large population and the importance of its economy. Here, three special runs with the Community Earth System Model (CESM) are used to project the changes in representative extreme precipitation indices (Rx1day, Rx5day, R95p, SDII) over East-Central Asia under the 1.5 °C and 2 °C Paris Agreement limits. The results indicate that Rx1day and Rx5day will increase by 28% and 15%, respectively, under the 1.5 °C warming level relative to the historical period (1971–2000). Most areas over East-Central Asia are projected to experience an accelerated increase in response to a further 0.5 °C warming. Specifically, humid areas (HAs) are projected to experience a greater increase in R95p annual days and area fraction, whereas arid and semiarid areas (ASAs) may have threefold higher risks. The proportion of extreme precipitation in total will increase ~10% in most HAs in response to the 0.5 °C additional warming. Holding global warming at 1.5 °C instead of 2 °C reduces the occurrence of R95p annual days by ~3 days/year in humid areas and ~1 day/year in ASAs. For SDII, most HAs will experience 0.2–0.6 mm/day and 0.2–0.4 mm/day increases in 1.5 °C or 2 °C warming limits, especially in Southeast China and the Himalayas. Therefore, limiting global warming to under 1.5 °C is beneficial to reducing the occurrence and associated impact of precipitation extremes in East-Central Asia.

Keywords Extreme precipitation · 1.5 °C and 2 °C warming limits · East-Central Asia · Arid and semiarid areas · Humid areas

Electronic supplementary material The online version of this article (https://doi.org/10.1007/s10584-020-02725-2) contains supplementary material, which is available to authorized users.

✉ Haipeng Yu
hpyu09@lzu.edu.cn

Extended author information available on the last page of the article

1 Introduction

As a meteorological phenomenon, extreme precipitation is responsible for many catastrophes and often causes disasters such as floods, which have great impacts on economic development, social stability, and people's livelihoods (Orlowsky and Seneviratne 2012; Yang et al. 2013; Scherrer et al. 2016). For instance, prolonged heavy precipitation led to the worst flooding in Pakistan's history in 2010, resulting in nearly 3000 deaths and affecting 20 million people. In Nara Prefecture of Japan, the 72-h rainfall record was broken in 2011, and that event resulted in 73 deaths and 20 missing people (Coumou and Rahmstorf 2012). It is crucial that the understanding of extreme precipitation changes be improved to better prepare, adapt, and mitigate the impacts of future events as the climate changes.

Due to the effect of land-sea thermal differences and human activities, East-Central Asia (10°–55°N, 60°–150°E) is one of the world's most vulnerable regions to extreme precipitation and its consequences (Zhai et al. 2005; Ren and Zhou 2014; Zhao et al. 2015; Lin et al. 2016; Guan et al. 2017; Zhou et al. 2018). Given the impacts of precipitation extremes, such extremes have become a topic of interest in recent years, with efforts to improve the understanding of historic changes and future projections especially prominent (Alexander et al. 2006; Kharin et al. 2013; Sillmann et al. 2013a, b). Since the Paris Agreement set a goal for limiting global warming below 2 °C and preferentially to 1.5 °C relative to pre-industrial levels, the variation in extreme climate conditions under future warming scenarios has also become an area of active research (Zhou and Chen 2015; Chen and Sun 2018; Dosio and Fischer 2018; King et al. 2018; Li et al. 2018; Wei et al. 2019). Lin et al. (2018) indicated that the average precipitation in China will increase by 11.6% (1.5 °C) and 13.3% (2 °C) compared with the 1976–2005 period. Chen and Sun (2017) pointed out that human influence will cause half of the occurrence probability increase of severe extremes in China. Zhang et al. (2018) indicated that 0.5 °C further warming would aggravate areal and population exposures to once-in-20-year extreme precipitation events by 25% in East Asia. Kusunoki (2017) pointed out that almost all eastern China areas are projected to experience more precipitation during 2079 to 2099. Other studies have also indicated that continued global temperature increases are projected to induce more extreme precipitation events in the future (Endo et al. 2017; Wang et al. 2017). There are several methods that can be used to form projections for climate extremes in different warmer worlds (e.g., the Coupled Model Intercomparison Project phase 5 (CMIP5) time-sampling and prescribed sea surface temperature (SST) simulations) (Mitchell et al. 2016; Schleussner et al. 2016; King et al. 2017). CMIP5 time sampling may utilize all four representative concentration pathways (RCPs) to generate a large sample of model years, but these are based on transient climates for low-end global warming limits, such as 1.5 °C and 2 °C. Atmosphere-only model simulations use prescribed SSTs, representing the recent period but with additional warming, to project future climates. However, there is an assumption that the recent period is representative of current climate variability and that coupled processes are not important to the extreme being investigated (Fischer et al. 2018). Here, we utilized three Community Earth System Model (CESM) experiments to analyze the spatiotemporal difference between the 1.5 °C and 2 °C warming limits and the recent historical period (Sanderson et al. 2017; Zhang et al. 2019a). To our knowledge, research on East-Central Asia extreme precipitation predictions using CESM 1.5 °C and 2 °C low warming runs (LWR) is scarce.

Precipitation in East-Central Asia is distributed unevenly owing to the influence of the monsoon and warm moist air from the ocean (Li et al. 2016; Xing et al. 2016). Monsoon areas have abundant precipitation, while inland areas, where there is a relative lack of water vapor

source, have little precipitation but high potential evapotranspiration. This difference in the mean climate state and interannual variability in the monsoon poses a challenge to water supply management (Huang et al. 2016a; Huang et al. 2017). The difference in background climate state and in precipitation extremes between these regions makes it necessary to analyze them separately. Thus, to be more precise and objective, we divide East-Central Asia into two subparts based on the aridity index (AI): humid areas (HAs) and arid and semiarid areas (ASAs). ASAs are defined as regions with an AI < 0.65 (Middleton and Thomas 1997). We utilized the AI provided by Feng and Fu (2013) and calculated for the historical period as a basis for the dry-wet division. For more details about the AI, please refer to (Scheff and Frierson 2014; Huang et al. 2016b).

In this study, we compared and analyzed four relevant and widely used extreme precipitation indices (Rx1day, Rx5day, R95p and SDII) (Karl et al. 1999; Peterson et al. 2001) and tried to answer the following three questions: (1) Will a remarkable difference appear in East-Central Asia under a 1.5 °C or 2 °C global warming future? (2) What is the difference due to a further 0.5 °C warming? (3) Are there differences in projections for ASAs and HAs?

2 Data and methods

2.1 Model data

We used the fully coupled climate model CESM released by the National Center for Atmospheric Research (NCAR) for our analysis of extreme precipitation projections under 1.5 °C and 2 °C global warming limits (Hurrell et al. 2013). The CESM LWR comprises a 10-member ensemble for 1.5 °C and 2 °C scenarios called 1 pt5 and 2 pt., respectively (Kay et al. 2015; Sanderson et al. 2016). By setting the radiative forcing of greenhouse gases, the global mean temperature relative to pre-industrial levels would rise monotonically to 1.5 °C (2 °C) by 2090–2100 under LWR 1 pt5 (2 pt.) scenarios. We also used RCP4.5 and RCP8.5 to provide further comparisons. The number of runs in the CESM models under the RCP4.5 scenarios is 15, and under the RCP8.5 scenarios, it is 30. Under RCPs, we define the 1.5 °C (2 °C) global warming level as the 11-year window based on the centers of chosen years (RCP4.5 and RCP8.5) when the 11-year mean temperature rises to 1.5 °C (2 °C) relative to pre-industrial levels. Therefore, the CESM LWR scenario represents the equilibrium climate response, while the RCPs represent transient climate response scenarios. The equilibrium climate response scenario means that the average global warming will stabilize at 1.5 °C or 2 °C by the end of the twenty-first century. Moreover, the carbon dioxide equivalence emission is matched with global temperature rises. For transient climate responses, such as RCP4.5 and RCP8.5, the global mean temperature would pass through 1.5 °C or 2 °C, and the final increase exceeds these two warming limits. This response might overestimate the temperature increase and cause some related influence. The dynamic and thermodynamic systems of the climate model simulation are not in equilibrium. Based on the climate model work principle, the equilibrium response scenario is considered more acceptable than the transient one. More details about CESM experiments can be found in Sanderson et al. (2017).

2.2 Extreme precipitation indices

Four extreme precipitation indices defined by the Expert Team for Climate Change Detection Monitoring and Indices (ETCCDI) were selected for analysis of the changes in extreme precipitation

events in warmer futures (Perkins et al. 2012; Donat et al. 2013; Perkins and Alexander 2013). Further details of the four selected extreme precipitation indices are provided in Table 1.

Rx1day and Rx5day are probably related to specific and possibly meteorologically distinct extreme precipitation events. R95p is useful in reflecting the absolute value change in total annual extreme precipitation. SDII is used to measure the intensity of precipitation on wet days. Together, these indices are useful in extending our understanding of the changing likelihood of extreme precipitation under 1.5 °C and 2 °C warming limits.

2.3 Probability ratio

The probability ratio (PR) is a metric to measure the probability of a specific event having changed. The formula and method come from the epidemiological field. Since being introduced to the climate change study area, PR has been used to detect the risk of the events occurring. The PR as a detection and attribution method represents the extent to which external forcing, such as global warming and the overall anthropogenic influence on the climate, affect extreme precipitation events (Fischer and Knutti 2015). The formula used is as shown in (1).

$$\mathrm{PR} = {}^{\mathrm{P_1}}/_{\mathrm{P_0}} \tag{1}$$

Here, P_0 refers to the extreme precipitation indices in a historical period (note that this is different from many event attribution studies, where an approximation for a pre-industrial climate is represented by P_0) and P_1 represents the probability of the event under a 1.5 °C or 2 °C warming future. The PR statistic can be considered an indicator for the change in the probability of the extreme precipitation indices: the reference value is 1.0, which would mean future likelihoods are the same as now. If PR > 1.0, the occurrence (for Rx1day and Rx5day) or intensity (for R95p and SDII) of precipitation extremes will increase, and vice versa (Stone and Allen 2005).

Table 1 Core set of four selected extreme indices recommended by the ETCCDI

Label	Name	Definition	Units
RX1day	Maximum 1 day precipitation	Let PR_{ij} be the daily precipitation amount on day i in period j. The maximum 1-day value for period j are $_{RX1day j=\max}(PR_{ij})$ It should be noted that the annual values are average monthly values.	mm
RX5day	Maximum consecutive 5 days precipitation	Let PR_{kj} be the precipitation amount for the 5-day interval ending k, period j. Then, maximum 5-day values for period j are $_{RX5day j=\max}(PR_{kj})$ It should be noted that the annual values are average monthly values.	mm
R95p	Annual total precipitation in very wet days	Let PR_{wj} be the daily precipitation amount on a wet day w in period i and let $PR_{wn}95$ be the 95th percentile of precipitation on wet days in the 1971–2000 period. If W represents the number of wet days in the period, then $R95_{pj} = \sum_{w=1}^{W} PR_{wj}(PR_{wj} = PR_{wn}95)$	mm
SDII	Simple daily intensity	Let PR_{wj} be the daily precipitation amount on wet days, PR >= 1 mm in period j. If W represents number of wet days in j, then: $SDII_j = \left(\sum_{w=1}^{W} PR_{wj}\right)/W$	mm/day

3 Results

3.1 Spatiotemporal change in the four indices

For Rx1day under 1.5 °C global warming, an obvious dividing line could be found in all four experiments (Fig. 1-4). It is worth mentioning that this boundary also separates ASAs from HAs. Southeast China and the Himalayas witness a rise of over 2 mm, based on the CESM LWR simulations, while the rest of the HAs experience a projected increase of 1–2 mm in a 1.5 °C world (Fig. 1(a)). The spatial patterns of RCP4.5 and RCP8.5 are similar to that in LWR. Nevertheless, the absolute increase in Southeast China is lower in the RCPs than in the LWR simulations (Fig. 1(c)(e)). There is consistency between Rx1day and Rx5day projections in their spatial pattern. There is a projected increase in Rx5day of over 6 mm in Southeast China and the Himalayas according to LWR, three times as much as for Rx1day (Fig. 2(a)).

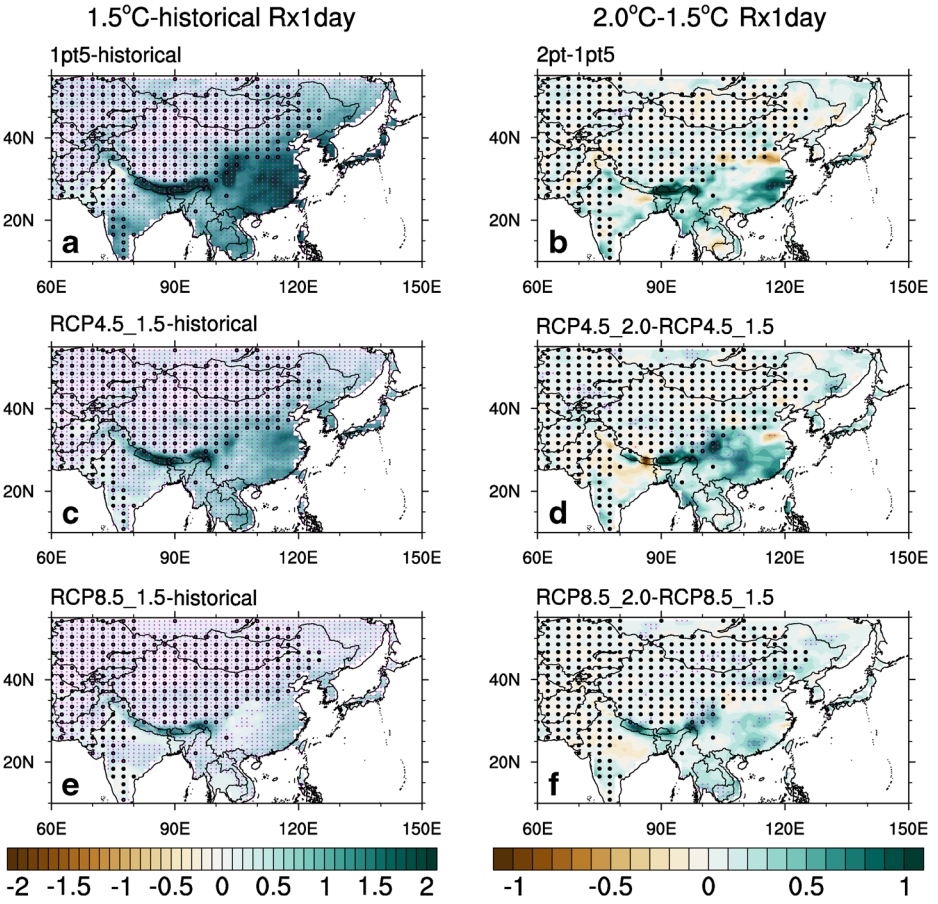

Fig. 1 Spatial changes in Rx1day (mm) in the 1.5 °C limits relative to (minus, the same below) the historical period for (a) 1 pt5, (c) RCP4.5, (e) RCP8.5. All the same but for 2 °C relative to 1.5 °C in (b) 2 pt., (d) RCP4.5, (f) RCP8.5. The black dotted parts represent ASAs. The red dotted parts represent the changes passing a 95% significance test

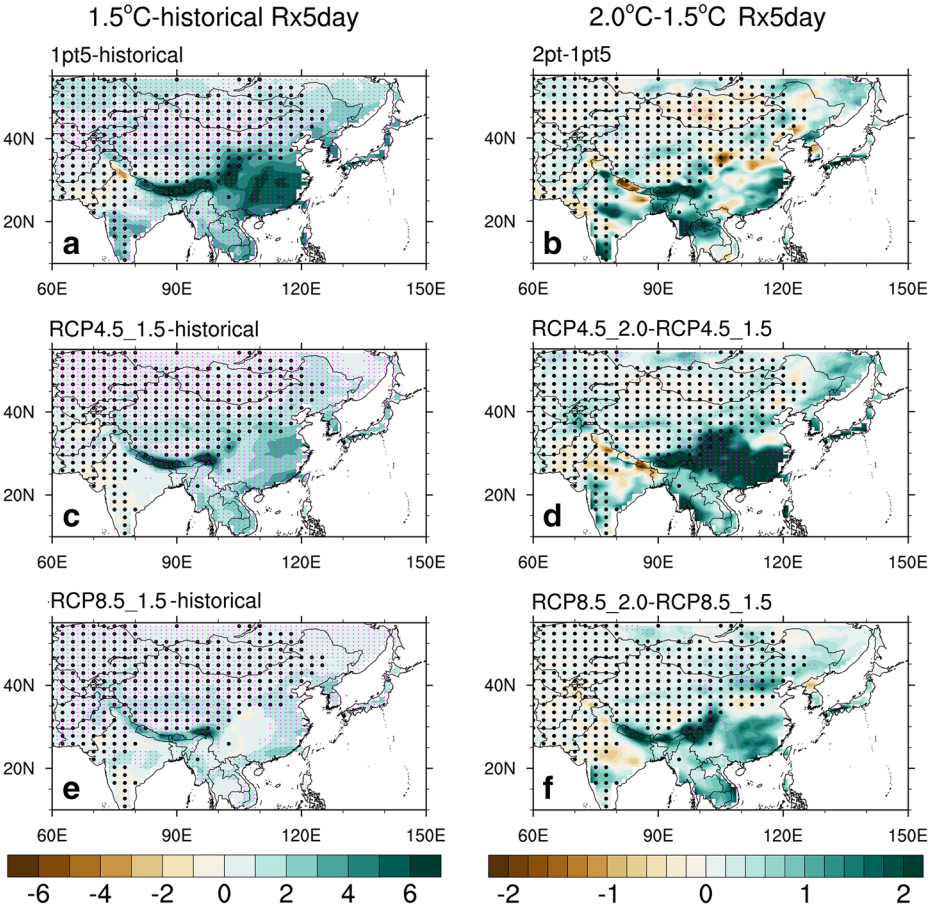

Fig. 2 The same as Fig. 1, but for Rx5day (mm)

The R95p index is projected to increase by over 200 mm under 1.5 °C global warming, such that a larger portion of the total annual precipitation in HAs, such as Southeast China and the Himalayas, is due to extreme rainfall (Fig. 3(a)). Likewise, RCP4.5 and RCP8.5 in Rx5day and R95p increase less compared with the LWR simulations (Fig. 2(c)(e) and Fig. 3(c)(e)). SDII represents the simple daily intensity of precipitation on wet days. If SDII increases in the future, the risk for extreme precipitation will be higher. From Fig. 4, we can see that most HAs are projected to experience a 0.5 mm/day increase under 1.5 °C relative to the historical period, whereas SDII in North India will decrease by approximately 0.5 mm/day (Fig. 4(a)(c)(e)).

For a further 0.5 °C warming in Rx1day, some regions (Southeast China and the Himalayas) still experience a modest increase of approximately 0.5–1 mm (Fig. 1(b)). Additionally, the difference in spatial pattern between the LWR and the other two experiments narrows (Fig. 1(d)(f)). Some regions, such as North China, North India and Pakistan, near the dry-wet transition zone, are simulated to experience a projected minor decrease in Rx1day. In these regions, increases in temperature and extreme precipitation are not positively related. This phenomenon might be induced by hydrologic cycle issues in the CESM. North India and Pakistan are located in the subtropical ASAs, which belongs to the sink branch of the Hadley

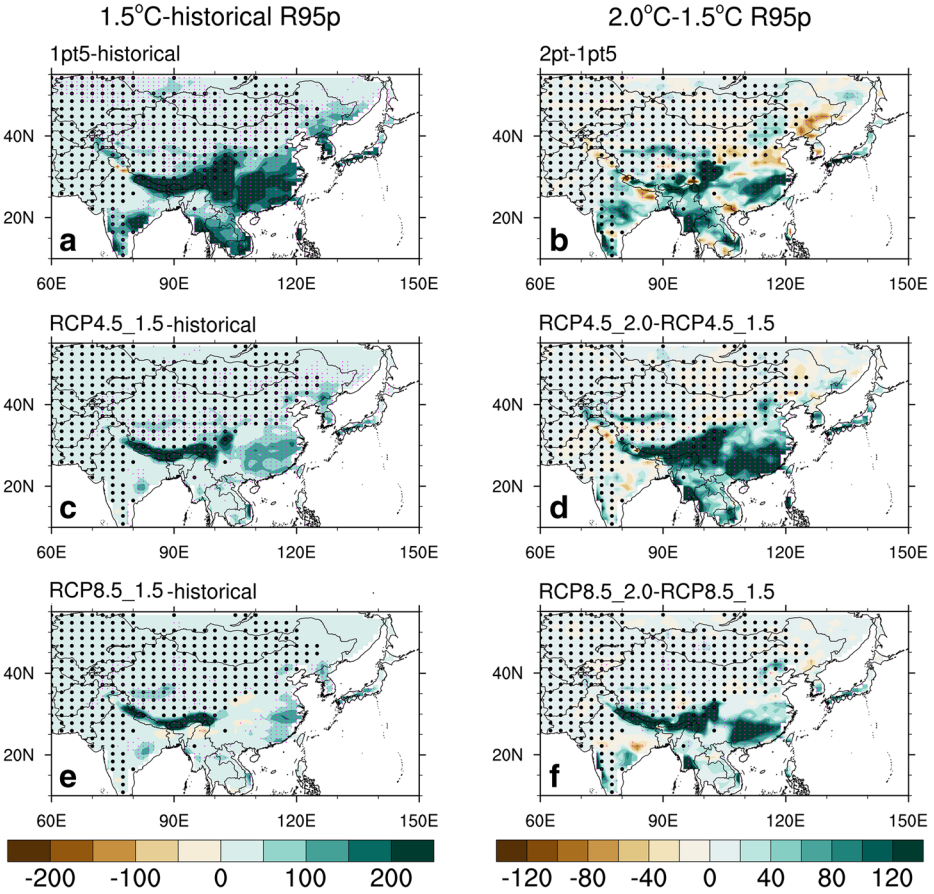

Fig. 3 The same as Fig. 1, but for R95p (mm)

circulation. An additional 0.5 °C warming from 1.5 °C to 2 °C is likely to cause more moisture divergence and then moisture content reduction (Zhang et al. 2019b). Thus, North India and Pakistan are projected to see decreasing trends in some extreme precipitation indices. The same phenomenon also occurs in Rx5day, but the amplitude is twice as high as that for Rx1day (Fig. 2(b)(d)(f)). Figure 3(b)(d)(f) illustrates that a further 0.5 °C warming is associated with an almost 100 mm increase in R95p in most HAs, illustrating a substantial benefit of keeping global warming to the more ambitious 1.5 °C Paris limit. Compared with the 200 mm rise under the 1.5 °C scenario relative to the historical period, a sharp acceleration appears in the 2 °C target relative to the 1.5 °C target. The increasing or decreasing tendency of SDII is still maintained in the mentioned areas (Fig. 4(b)(d)(f)).

The spatiotemporal change in percentage is different from that in absolute value mentioned before (Figs. S1–S4). The change in the absolute value of extreme precipitation in ASAs is relatively small compared with that in HAs. However, under the 1.5 °C and 2 °C warming futures, there will be a sharp increase in the extreme precipitation percentage in most ASAs. The specific increases in ASAs in Rx1day, Rx5day, R95p and SDII under 1.5 °C relative to the historical period are 20–40%, 10–30%, 100–200%, and 5–15%, respectively. The

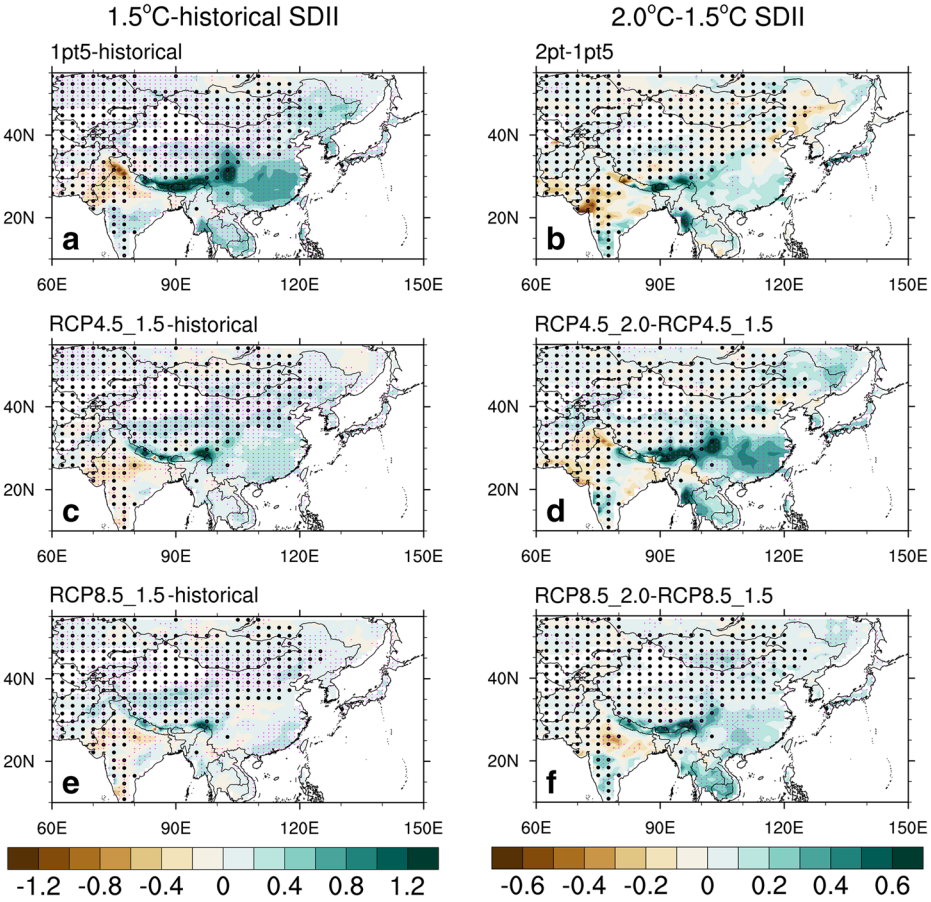

Fig. 4 The same as Fig. 1, but for SDII (mm/day)

additional 0.5 °C warming provides a further 5–10% increase in both Rx1day and Rx5day. For R95p, the average increase is 30–50%. SDII in most ASAs is projected to experience a 2–4% increase, although North India and Pakistan will witness a slight decrease. In summary, most ASAs may experience more extreme precipitation events in the warming future.

3.2 Probability ratio change in Rx1day and Rx5day

The absolute value changes in extreme precipitation under the 1.5 °C and 2 °C warming limits show how rainfall extremes are projected to alter in the future, but PR values provide likelihood changes in extremes that help inform decision-making. Figure 5 shows the statistical distribution of PR values by gridbox in Rx1day and Rx5day under the 1.5 °C and 2 °C global warming limits relative to the historical period. According to Fig. 5(a),(b), only 5% of all grid points see a decrease in Rx1day, and the rest of the area is projected to experience increases in this index, especially for the changes higher than the 90th percentile, which rise at a higher rate. For Rx5day, the proportion of all grid points that experience a PR below one

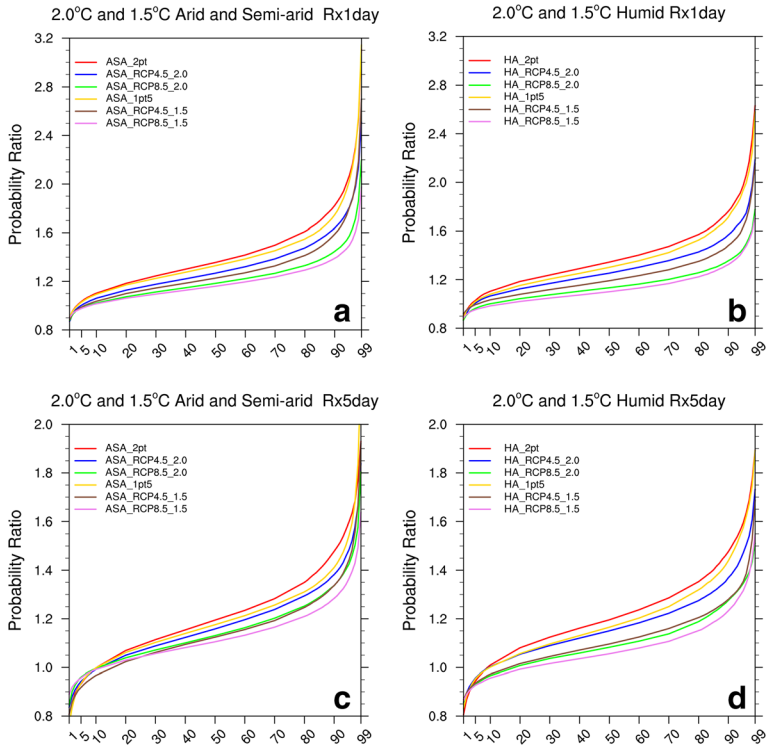

Fig. 5 (a) PR values in Rx1day in ASAs under 2 °C and 1.5 °C limits relative to the historical period. The x-axis represents the percentile thresholds based on the historical period. The method is as follows: First, we calculate the Rx1day in the historical period (average of 30 years) and under the 1.5 °C warming condition in each grid point and obtain two three-dimensional arrays (month, latitude, longitude), both of which are 12, 47, 73, respectively. Then, we calculate PR values using the two arrays in each grid point and set grid points in humid areas as missing values. After that, we convert this new three-dimensional array of PR into a one-dimensional array in ascending sequence. Finally, we set the percentile thresholds and draw the figures. (b), (c), and (d) are the same as (a) but represent Rx1day in HAs, Rx5day in ASAs, and Rx5day in HAs, respectively

increases from 5% to 10%. This is unsurprising given that Rx5day is a less extreme rainfall index than Rx1day and tends to exhibit behavior more similar to the mean. As shown in Fig. 5, there is almost no distinction between the 1.5 °C and 2 °C representative lines when considering the same experiment. However, obvious differences appear between the three experiments (LWR, RCP4.5, RCP8.5). The CESM LWR simulation rises at the highest rate, followed by RCP4.5, and RCP8.5 presents the lowest rate. The increase in the indices at high percentiles is higher in the LWR simulations than under the RCPs. This indicates that the influence might be different between transient and quasi-equilibrium simulations. ASAs are projected to experience greater relative increases in the upper tail for these indices than HAs. This suggests that ASAs may need to prepare for greater risks from extreme precipitation events under global warming.

For 1.5 °C relative to the historical period, greater PR values are simulated in East-Central Asia (with PR in most regions of 1.0–1.5) (Fig. 6(a)(c)(e)). There is no monotonic increase in Rx1day under a further 0.5 °C warming. Central Asia and North India, which are projected to experience substantial increases in precipitation

extremes under warming to 1.5 °C, are projected to experience slight decreases between 1.5 °C and 2 °C global warming. This again illustrates that warming and precipitation increases are not simply positively correlated. However, most regions still show positive correlations between temperature and extreme precipitation changes (Fig. 6(b)(d)(f)). The spatial pattern of Rx5day is similar to that of Rx1day but with smaller PR values (Fig. 7).

3.3 Further changes in R95p

In general, the higher the extreme precipitation proportion, the greater the probability risks. Figure 8 provides the changes in R95p as a percentage of total precipitation, and we see that the increases in magnitude exceed 10% in HAs (Fig. 8(a)). Under RCP4.5 and RCP 8.5, Southeast China and the Himalayas also experience increases in the proportion of extreme precipitation, but these are lower than those projected by

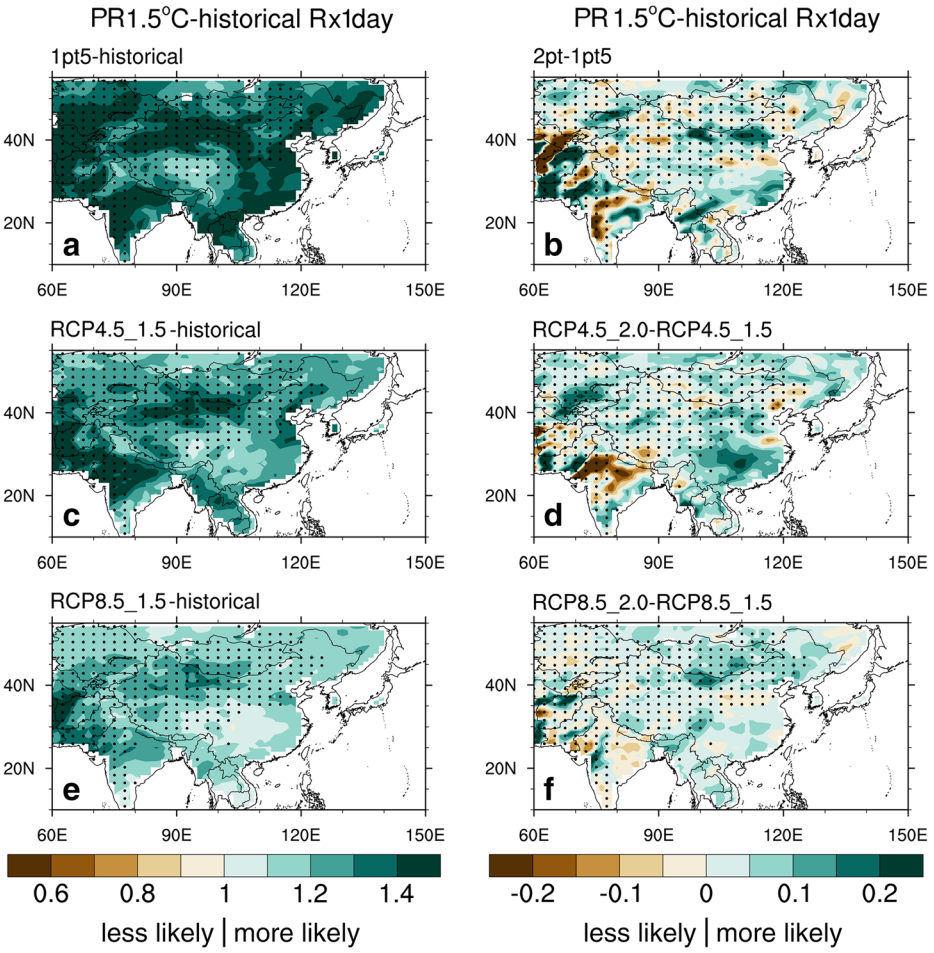

Fig. 6 PR spatial changes in Rx1day in the 1.5 °C limits relative to the historical period for (a) 1 pt5, (c) RCP4.5, (e) RCP8.5. All the same but for 2 °C relative to 1.5 °C in (b) 2 pt., (d) RCP4.5, (f) RCP8.5. The black dotted parts represent ASAs

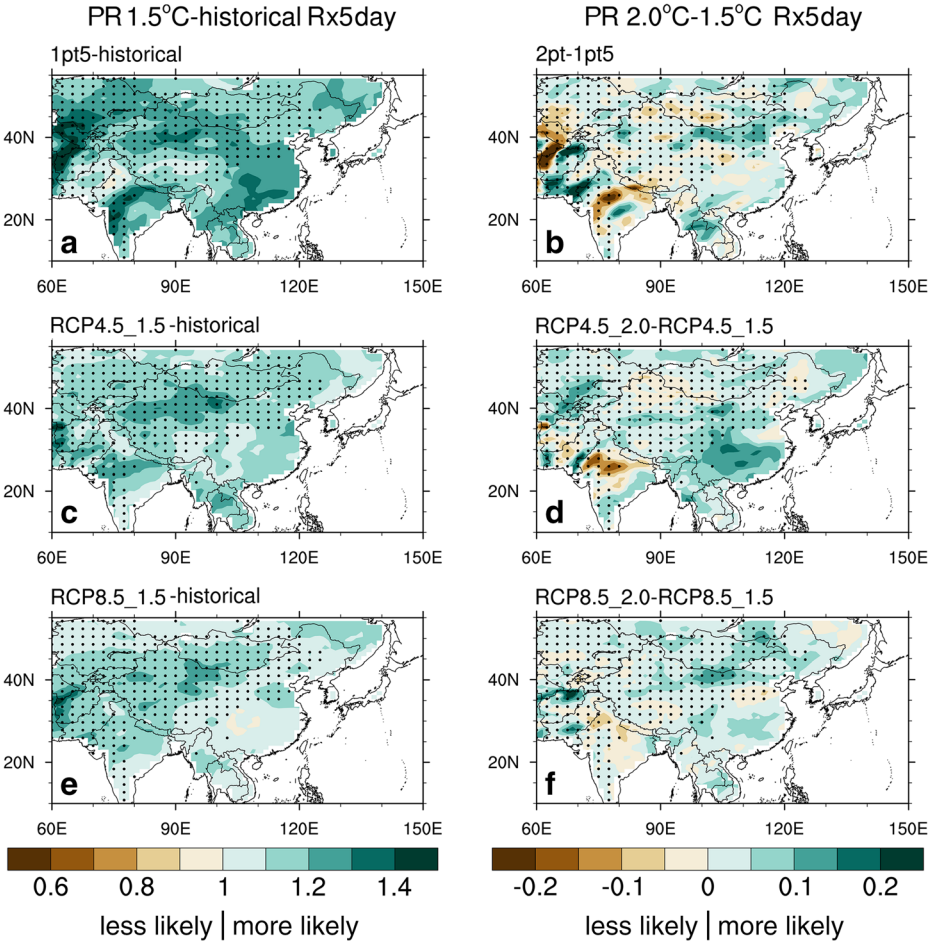

Fig. 7 The same as Fig. 6, but for Rx5day

the LWR. Other HAs have less obvious variation in R95p changes under the RCPs compared with the results of the LWR (Fig. 8(c)(e)). Likewise, there is little change in ASAs based on the three experiments. Increasing warming by 0.5 °C appears to be a double-edged sword that would cause some regions (Southeast China and the Himalayas) to experience increased extreme precipitation and other regions (North China and North India) to experience spatially inhomogeneous changes and perhaps even decreases (Fig. 8(b)(d)(f)).

We use the R95p annual days change to describe the variation intensity and R95p area fraction change for the variation range. R95p annual days means the count of total annual days that meet the definition of R95p. The R95p area fraction indicates the variation of the R95p percentage shift to positive or negative. Under the background of extreme precipitation increasing, R95p annual days in HAs increase by 10.8 days, 3.8 days, and 1.5 days in the 1.5 °C limits and increase by 13.1 days, 8.4 days, and 4.2 days in the 2 °C limits according to LWR, RCP4.5, and RCP8.5, respectively. Coincident with spatial pattern changes, the annual day variation in ASAs is not obvious (Table S1). From the perspective of the R95p area fraction, R95p in most HAs is projected to see increases both under the 1.5 °C and the 2 °C

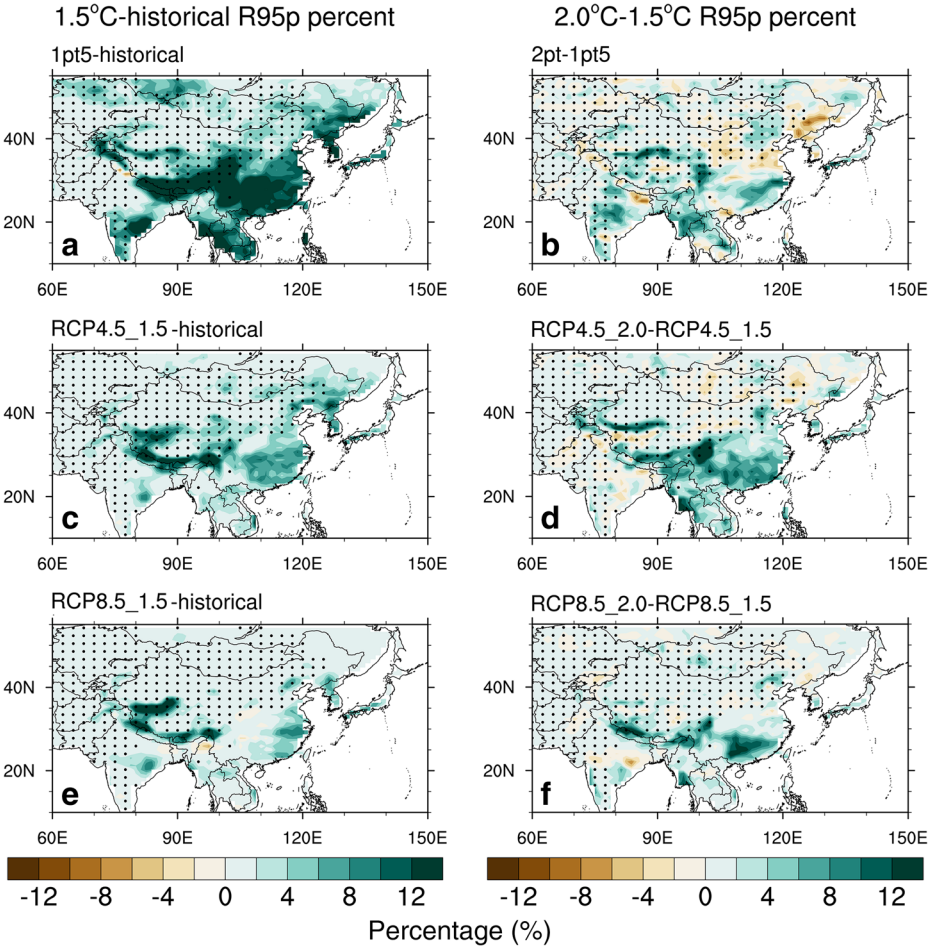

Fig. 8 Spatial changes in R95p as a percentage of total precipitation in the 1.5 °C limits relative to the historical period for (a) 1 pt5, (c) RCP4.5, (e) RCP8.5. All the same but for 2 °C relative to 1.5 °C for (b) 2 pt., (d) RCP4.5, (f) RCP8.5. The black dotted parts represent ASAs

warming limits. In contrast, only half of ASAs are expected to witness more R95p, and the proportion of R95p in ASAs increases only slightly under 0.5 °C further warming (Table S2).

4 The mechanisms and uncertainty of the results

From the CESM model's extreme precipitation prediction results, we can conclude that along with the mean temperature increase, the extreme precipitation response is uneven in different areas. In the 1.5 °C and 2 °C warming future, ASAs will tend to experience a greater mean temperature increase than HAs due to the differences in vegetation cover, types of clouds, and anthropogenic aerosols (Huang et al. 2017). The lower vegetation cover in ASAs leads to lower transpiration rates, resulting in higher surface air temperatures. The thick low clouds in HAs can effectively reflect shortwave sunlight, and their low cloud tops result in limited

longwave warming effects. In contrast, most cirrus clouds in ASAs reflect less sunlight to the top atmosphere but absorb more atmospheric counter radiation, leading to a sharp regional temperature increase. Moreover, anthropogenic aerosols, which are likely to cool down the surface, are less abundant in ASAs than in HAs. Thus, due to the intensifying warming effect, the ASAs will bear higher extreme precipitation event risks, and the extreme precipitation percentage variation changes in most ASAs are projected to be higher than those in the HAs. For the hydrologic cycle, HAs are likely to witness more increases in moisture convergence and then more total precipitation, while the moisture divergence in ASAs is anomalous (Zhang et al. 2019b). More base precipitation and moisture convergence in the warmer world drive HAs to experience more total extreme precipitation increases.

The CESM is released by NCAR and consists of several component models and a coupler. Each module is independent, and modules are connected by a coupler (Kay et al. 2015). Although that design may reduce model errors as much as possible, it still has some internal errors that are hard to eliminate because of the simulation deviation of the model from the actual atmospheric motion state and errors in coupling. Moreover, some physical processes, parameterized schemes and dynamic frameworks must be constantly improved. The CESM LWR begins from a slightly different initial atmospheric state (created by randomly perturbing temperatures at the level of round-off error). However, there are still some differences among those runs considering extreme precipitation indices. RCP4.5 and RCP8.5 are transient scenarios, and the response to 1.5 °C or 2 °C warming limits is not in equilibrium. This will result in some overestimation of the temperature increase and cause some related influence, as mentioned in the model data. Despite these problems, the three special CESM runs used in our paper reveal that extreme precipitation will increase regardless of intensity or occurrence under the background of global warming in the future. This is in line with most other climate models and our knowledge. To better understand the reason for these uneven changes and their underlying physical mechanisms, more specific global and regional climate models need to be tested in further studies.

5 Summary and conclusions

We utilized four climate prediction experiments from CESM to investigate changes in extreme precipitation under the 1.5 °C and 2 °C global warming limits over East-Central Asia. Under the 1.5 °C warming limits, extreme precipitation is projected to increase in almost all regions, especially in Southeast China and the Himalayas. With a further 0.5 °C warming, most regions are projected to experience a further increase in extreme precipitation, although it is not a linear increase. Overall, there will be more extreme precipitation over East-Central Asia under global warming.

According to the LWR, Southeast China and the Himalayas will witness over 2 mm and 6 mm increases in Rx1day and Rx5day in the 1.5 °C warming future, respectively. However, RCP4.5 and RCP8.5 suggest only a slight increase (perhaps due to a difference between transient and quasi-equilibrium responses). For the 2 °C limit relative to 1.5 °C, the response of HAs to temperature rise is almost positive, while some ASAs, such as North India, North China, and Northeast Mongolia, indicate a moderate decrease.

The PR of Rx1day and Rx5day will grow exponentially with increasing percentile thresholds, indicating that the most intense extreme precipitation events will occur more frequently in the warming future. It is worth mentioning that the slope of PR in ASAs will be greater than that in HAs, which means a higher relative increase in risk. Considering that ASAs are less

resistant and more vulnerable to storms and floods, extreme precipitation events may cause more disasters here unless adequate adaptation plans are put in place.

There is projected to be an over 200-mm increase in the amplitude of R95p in a 1.5 °C future and a further 100-mm increase in 2 °C relative to 1.5 °C in Southeast China and the Himalayas. The proportion of R95p in total precipitation will also have a modest increase of approximately 10–20% in the regions previously mentioned. Nevertheless, ASAs are expected to experience spatially inhomogeneous changes in the contribution of extreme precipitation to total precipitation. This difference is also reflected in the changes in R95p annual days and the percentage of R95p area. Approximately a 5-day increase under 1.5 °C and an 8-day increase under 2 °C are expected to appear in HAs. Half of the ASAs locations are expected to experience an increase and half a decrease in R95p annual days. Likewise, only HAs are expected to experience large increases in the R95p area fraction.

For the changes in SDII, most HAs will witness 0.4–0.8 mm/day (in 1.5 °C relative to the historical period) and 0.2–0.4 mm/day (in 2 °C relative to 1.5 °C) increases. North India and Pakistan are projected to experience decreases, and most ASAs will see SDII increases in terms of values and percentiles.

Acknowledgements This work was jointly supported by the National Natural Science Foundation of China (41705077 and 41630426) and the National Key Research and Development Program of China (2017YFC1502305). ADK was funded by the Australian Research Council (DE180100638). The authors acknowledge the NCAR for releasing the CESM low-warming experiment products and the data were acquired from http://www.cesm.ucar.edu/experiments/1.5-2.0-targets.html. The authors thank the two anonymous reviewers for their valuable suggestions.

References

Alexander LV, Zhang X, Peterson TC, Caesar J, Gleason B, Tank AMGK et al (2006) Global observed changes in daily climate extremes of temperature and precipitation. J Geophys Res-Atmos 111:D05109. https://doi.org/10.1029/2005JD006290

Chen HP, Sun JQ (2017) Contribution of human influence to increased daily precipitation extremes over China. Geophys Res Lett 44(5):2436–2444. https://doi.org/10.1002/2016GL072439

Chen HP, Sun JQ (2018) Projected changes in climate extremes in China in a 1.5°C warmer world. Int J Climatol 38(9):3607–3617. https://doi.org/10.1002/joc.5521

Coumou D, Rahmstorf S (2012) A decade of weather extremes. Nat Clim Chang 2:491–496. https://doi.org/10.1038/NCLIMATE1452

Donat MG, Alexander LV, Yang H, Durre I, Vose R, Dunn RJH et al (2013) Updated analyses of temperature and precipitation extreme indices since the beginning of the twentieth century: the HadEX2 dataset. J Geophys Res-Atmos 118:2098–2118. https://doi.org/10.1002/jgrd.50150

Dosio A, Fischer EM (2018) Will half a degree make a difference robust projections of indices of mean and extreme climate in Europe under 1.5°C, 2°C, and 3°C global warming. Geophys Res Lett 45:935–944. https://doi.org/10.1002/2017GL076222

Endo H, Kitoh A, Mizuta R, Ishii M (2017) Future changes in precipitation extremes in East Asia and their uncertainty based on large ensemble simulations with a high-resolution AGCM. SOLA 13(0):7–12. https://doi.org/10.2151/sola.2017-002

Feng S, Fu Q (2013) Expansion of global drylands under a warming climate. Atmos Chem Phys 13:10081–10094. https://doi.org/10.5194/acp-13-10081-2013

Fischer EM, Beyerle U, Schleussner CF, King AD, Knutti R (2018) Biased estimates of changes in climate extremes from prescribed SST simulations. Geophys Res Lett 45(16):8500–8509. https://doi.org/10.1029/2018GL079176

Fischer EM, Knutti R (2015) Anthropogenic contribution to global occurrence of heavy-precipitation and high-temperature extremes. Nat Clim Chang 5:560–564. https://doi.org/10.1038/nclimate2617

Guan YH, Zheng FL, Zhang XC, Wang B (2017) Trends and variability of daily precipitation and extremes during 1960-2012 in the Yangtze River basin, China. Int J Climatol 37:1282–1298. https://doi.org/10.1002/joc.4776

Huang JP, Ji MX, Xie YK, Wang SS, He YL, Ran JJ (2016b) Global semi-arid climate change over last 60 years. Clim Dyn 46:1131–1150. https://doi.org/10.1007/s00382-015-2636-8

Huang JP, Yu HP, Dai AG, Wei Y, Kang LT (2017) Drylands face potential threat under 2°C global warming target. Nat Clim Chang 7(6):417–422. https://doi.org/10.1038/NCLIMATE3275

Huang JP, Yu HP, Guan XD, Wang GY, Guo RX (2016a) Accelerated dryland expansion under climate change. Nat Clim Chang 6(2):166–171. https://doi.org/10.1038/NCLIMATE2837

Hurrell JW, Holland MM, Gent PR, Ghan S, Kay JE, Kushner PJ et al (2013) The community earth system model a framework for collaborative research. Bull Am Meteorol Soc 94:1339–1360. https://doi.org/10.1175/BAMS-D-12-00121.1

Karl TR, Nicholls N, Ghazi A (1999) CLIVAR/GCOS/WMO workshop on indices and indicators for climate extremes: workshop summary. Clim Chang 42:3–7. https://doi.org/10.1023/A:1005491526870

Kay JE, Deser C, Phillips A, Mai A, Hannay C, Strand G et al (2015) The community earth system model (CESM) large ensemble project: a community resource for studying climate change in the presence of internal climate variability. Bull Am Meteorol Soc 96:1333–1349. https://doi.org/10.1175/BAMS-D-13-00255.1

Kharin VV, Zwiers FW, Zhang X, Wehner M (2013) Changes in temperature and precipitation extremes in the CMIP5 ensemble. Clim Chang 119:345–357. https://doi.org/10.1007/s10584-013-0705-8

King AD, Karoly DJ, Henley BJ (2017) Australian climate extremes at 1.5°C and 2°C of global warming. Nat Clim Chang 7(6):412–416. https://doi.org/10.1038/NCLIMATE3296

King AD, Knutti R, Uhe P, Mitchell DM, Lewis SC, Arblaster JM, Freychet N (2018) On the linearity of local and regional temperature changes from 1.5°C to 2°C of global warming. J Clim 31(18):7495–7514. https://doi.org/10.1175/JCLI-D-17-0649.1

Kusunoki S (2017) Future changes in precipitation over East Asia projected by the global atmospheric model MRI-AGCM3.2. Clim Dyn 51:4601–4617. https://doi.org/10.1007/s00382-016-3499-3

Li DH, Zhou TJ, Zou LW, Zhang WX, Zhang LX (2018) Extreme high-temperature events over East Asia in 1.5°C and 2°C warmer futures analysis of NCAR CESM low-warming experiments. Geophys Res Lett 45:1541–1550. https://doi.org/10.1002/2017GL076753

Li Q, Zhang RH, Wang Y (2016) Interannual variation of the wintertime fog-haze days across central and eastern China and its relation with east Asian winter monsoon. Int J Climatol 36:346–354. https://doi.org/10.1002/joc.4350

Lin L, Wang ZL, Xu YY, Fu Q (2016) Sensitivity of precipitation extremes to radiative forcing of greenhouse gases and aerosols. Geophys Res Lett 43(18):9860–9868. https://doi.org/10.1002/2016GL070869

Lin L, Wang ZL, Xu YY, Zhang XY, Zhang H, Dong WJ (2018) Additional intensification of seasonal heat and flooding extreme over China in a 2°C warmer world compared to 1.5°C. Earths Future 6(7):968–978. https://doi.org/10.1029/2018EF000862

Middleton NJ, Thomas DSG (1997) World atlas of desertification, 2nd edn. Arnold, London

Mitchell D, Heaviside C, Vardoulakis S, Huntingford C, Masato G, Guillod BP et al (2016) Attributing human mortality during extreme heat waves to anthropogenic climate change. Environ Res Lett 11(7):074006. https://doi.org/10.1088/1748-9326/11/7/074006

Orlowsky B, Seneviratne SI (2012) Global changes in extreme events: regional and seasonal dimension. Clim Chang 110:669–696. https://doi.org/10.1007/s10584-011-0122-9

Perkins SE, Alexander LV (2013) On the measurement of heat waves. J Clim 26:4500–4517. https://doi.org/10.1175/JCLI-D-12-00383.1

Perkins SE, Alexander LV, Nairn JR (2012) Increasing frequency, intensity and duration of observed global heatwaves and warm spells. Geophys Res Lett 39:L20714. https://doi.org/10.1029/2012GL053361

Peterson TC et al. (2001) Report on the activities of the Working Group on Climate Change Detection and Related Rapporteurs 1998-2001. WMO, Rep. WCDMP-47, WMO-TD 1071, Geneve, Switzerland, p 143

Ren GY, Zhou YQ (2014) Urbanization effect on trends of extreme temperature indices of national stations over mainland China, 1961-2008. J Clim 27:2340–2360. https://doi.org/10.1175/JCLI-D-13-00393.1

Sanderson BM, O'Neill B, Tebaldi C (2016) What would it take to achieve the Paris temperature targets? Geophys Res Lett 43:7133–7142. https://doi.org/10.1002/2016GL069563

Sanderson BM, Xu YY, Tebaldi C, Wehner M, O'Neill B, Jahn A et al (2017) Community climate simulations to assess avoided impacts in 1.5°C and 2°C futures. Earth System Dynamics 8:827–847. https://doi.org/10.5194/esd-8-827-2017

Scheff J, Frierson DMW (2014) Scaling potential evapotranspiration with greenhouse warming. J Clim 27:1539–1558 https://doi.org/10.1175/JCLI-D-13-00233.1

Scherrer SC, Fischer EM, Posselt R, Liniger MA, Croci-Maspoli M, Knutti R (2016) Emerging trends in heavy precipitation and hot temperature extremes in Switzerland. J Geophys Res-Atmos 121:2626–2637. https://doi.org/10.1002/2015JD024634

Schleussner CF, Lissner TK, Fischer EM, Wohland J, Perrette M, Golly A et al (2016) Differential climate impacts for policy-relevant limits to global warming: the case of 1.5°C and 2°C. Earth System Dynamics 7(2):327–351. https://doi.org/10.5194/esd-7-327-2016

Sillmann J, Kharin VV, Zhang X, Zwiers FW, Bronaugh D (2013a) Climate extremes indices in the CMIP5 multimodel ensemble: part 1. Model evaluation in the present climate *Journal of Geophysical Research-Atmospheres* 118:1716–1733. https://doi.org/10.1002/jgrd.50203

Sillmann J, Kharin VV, Zhang X, Zwiers FW, Bronaugh D (2013b) Climate extremes indices in the CMIP5 multimodel ensemble: part 2. Future climate projections *Journal of Geophysical Research-Atmospheres* 118: 2473–2493. https://doi.org/10.1002/jgrd.50188

Stone DA, Allen MR (2005) The end-to-end attribution problem: from emissions to impacts. Clim Chang 71: 303–318. https://doi.org/10.1007/s10584-005-6778-2

Wang ZL, Lin L, Zhang XY, Zhang H, Liu LK, Xu YY (2017) Scenario dependence of future changes in climate extremes under 1.5°C and 2°C global warming. Sci Rep 7:46432. https://doi.org/10.1038/srep46432

Wei Y, Yu HP, Huang JP, Zhou TJ, Zhang M, Ren Y (2019) Drylands climate response to transient and stabilized 2°C and 1.5°C global warming targets. Clim Dyn 53(3–4):2375–2389. https://doi.org/10.1007/s00382-019-04860-8

Xing W, Wang B, Yim SY (2016) Peak-summer east Asian rainfall predictability and prediction part I: Southeast Asia. Clim Dyn 47:1–13. https://doi.org/10.1007/s00382-014-2385-0

Yang L, Villarini G, Smith JA, Tian FQ, Hu HP (2013) Changes in seasonal maximum daily precipitation in China over the period 1961-2006. Int J Climatol 33:1646–1657. https://doi.org/10.1002/joc.3539

Zhai PM, Zhang XB, Wan H, Pan XH (2005) Trends in total precipitation and frequency of daily precipitation extremes over China. J Clim 18:1096–1108. https://doi.org/10.1175/JCLI-3318.1

Zhang M, Yu HP, Huang JP, Wei Y, Liu XY, Zhang TH (2019a) Comparison of extreme temperature response to 0.5°C additional warming between dry and humid regions over East-Central Asia. Int J Climatol 39:3348–3364. https://doi.org/10.1002/joc.6025

Zhang WX, Zhou TJ, Zou LW, Zhang LX, Chen XL (2018) Reduced exposure to extreme precipitation from 0.5°C less warming in global land monsoon regions. Nat Commun 9:3153. https://doi.org/10.1038/s41467-018-05633-3

Zhang W, Zhou T, Zhang L, Zou L (2019b) Future intensification of the water cycle with an enhanced annual cycle over global land monsoon regions. J Clim 32:5437–5452. https://doi.org/10.1175/jcli-d-18-0628.1

Zhao GJ, Huang G, Wu RG, Tao WC, Gong HN, Qu X, Hu KM (2015) A new upper-level circulation index for the east Asian summer monsoon variability. J Clim 28(24):9977–9996. https://doi.org/10.1175/JCLI-D-15-0272.1

Zhou SJ, Huang G, Huang P (2018) Changes in the east Asian summer monsoon rainfall under global warming: moisture budget decompositions and the sources of uncertainty. Clim Dyn 51(4):1363–1373. https://doi.org/10.1007/s00382-017-3959-4

Zhou TJ, Chen XL (2015) Uncertainty in the 2°C warming threshold related to climate sensitivity and climate feedback. Journal of Meteorological Research 29(6):884–895. https://doi.org/10.1007/s13351015-5036-4

Publisher's note Springer Nature remains neutral with regard to jurisdictional claims in published maps and institutional affiliations.

Affiliations

Meng Zhang [1,2] · Haipeng Yu [1,3] · Andrew D. King [4] · Yun Wei [2] · Jianping Huang [5] · Yu Ren [2]

Meng Zhang
zhangm2012@lzu.edu.cn

Andrew D. King
andrew.king@unimelb.edu.au

Yun Wei
weiy16@lzu.edu.cn

Jianping Huang
hjp@lzu.edu.cn

Yu Ren
yren15@lzu.edu.cn

[1] Key Laboratory of Land Surface Process and Climate Change in Cold and Arid Regions, Northwest Institute of Eco-Environment and Resources, Chinese Academy of Sciences, Lanzhou, China

[2] Key Laboratory for Semi-Arid Climate Change of the Ministry of Education, College of Atmospheric Sciences, Lanzhou University, Lanzhou, China

[3] Key Laboratory of Arid Climatic Change and Disaster Reduction in Gansu Province, Key Open Laboratory of Arid Climatic Change and Disaster Reduction in CMA, Institute of Arid Meteorology, CMA, Lanzhou, China

[4] ARC Centre of Excellence for Climate Extremes, School of Earth Sciences, University of Melbourne, Melbourne 3010, Australia

[5] Collaborative Innovation Center for Western Ecological Safety, Lanzhou University, Lanzhou, China